

# Emergence of second-order coherence in the superradiant emission from a free-space atomic ensemble

Giovanni Ferioli,<sup>1,\*</sup> Igor Ferrier-Barbut,<sup>2,†</sup> and Antoine Browaeys<sup>2,‡</sup>

<sup>1</sup>*Dipartimento di Fisica e Astronomia, Universit a degli studi di Firenze, Via G. Sansone 1, 50019 Sesto Fiorentino, Italy*

<sup>2</sup>*Universit  Paris-Saclay, Institut d'Optique Graduate School,  
CNRS, Laboratoire Charles Fabry, 91127, Palaiseau, France*

(Dated: October 14, 2024)

We investigate the evolution of the second-order temporal coherence during the emission of a superradiant burst by an elongated cloud of cold Rb atoms in free space. To do so, we measure the two-times intensity correlation function  $g_N^{(2)}(t_1, t_2)$  following the pulsed excitation of the cloud. By monitoring  $g_N^{(2)}(t, t)$  during the burst, we observe the establishment of second-order coherence, and contrast it with the situation where the cloud is initially prepared in a steady state. We compare our findings to the predictions of the Dicke model, using an effective atom number to account for finite size effects, finding that the model reproduces the observed trend at early time. For longer times, we observe a subradiant decay, a feature that goes beyond Dicke's model. Finally, we measure the  $g_N^{(2)}(t_1, t_2)$  at different times and observe the appearance of anti-correlations during the burst, that are not present when starting from a steady state.

It is well known that a single excited two-level emitter decays exponentially, with a time constant related to the linewidth of the transition. This situation can be drastically modified if many emitters are coupled to a common radiation mode, as is the case when placed in an optical cavity or if they are confined within a subwavelength-sized volume. There, the system emits a short burst of photons with an initial increase of the emission rate. The origin of this superradiant (or superfluorescent) burst, predicted by R. H. Dicke in 1954 [1, 2], stems from a progressive phase locking of the atomic dipoles. This happens spontaneously during the decay process, and results into the  $N^2$  scaling of the largest emission rate of the ensemble, a behavior considered a fingerprint of Dicke's superradiance.

Starting from the first experimental demonstrations in thermal gases of atoms and molecules [3–5], superradiant bursts have been observed in many experimental platforms [2], including nuclei [6], artificial atoms [7] and recently a in cascaded atomic system [8]. However, most of these works measured the photon emission rate while the investigation of other defining characteristics of the emitted light, such as first and second-order temporal and spatial coherence have been addressed only recently in few cases [9–12]. Beyond its fundamental interest, exploring the statistical properties of a system featuring superradiant correlations will be useful to characterize a novel class of superradiant lasers [13–16] or other non-classical sources of light [17, 18].

Here, we investigate the establishment of second-order temporal coherence during the emission of a superradiant burst [11, 19] by an elongated cloud of laser cooled  $^{87}\text{Rb}$  atoms in free space. To do so, we measure the two-times intensity correlation function  $g_N^{(2)}(t_1, t_2)$  of the emitted light during the decay following the excitation of the cloud. Our results present strong similarities with a recent experiment carried out in an atomic ensemble chirally coupled to the mode of a nano-fiber [12]. Here instead, the cooperative emission occurs symmetrically in two diffraction modes

with opposite directions along the long axis of the cloud. Our findings confirm that the establishment of temporal correlations is a generic feature of Dicke superradiance, independent of the specific symmetries characterizing the atomic ensemble. We also find that, for a part of the emission, the experimental photon emission rate and equal-time correlation function are quantitatively reproduced by the Dicke model, introducing an effective atom number to account for the finite size extension of the cloud [2, 20]. However, some observed features are, as expected, beyond the Dicke model, which fails for instance to reproduce the observed subradiant decay at long time. This calls for a more sophisticated theoretical model able to include finite size effects as well as photon-mediated interaction between the emitters [11, 21–24].

Our experimental setup is sketched in Fig. 1(a) [25]. We load up to  $\simeq 3000$   $^{87}\text{Rb}$  atoms in a  $2.5\mu\text{m}$ -waist optical trap using gray molasses. The resulting elongated atomic cloud has a typical temperature of  $200\mu\text{K}$ , a calculated radial r.m.s. size  $\ell_{\text{rad}} \approx 0.6\lambda$  and a measured axial r.m.s. size  $\ell_{\text{ax}} \simeq 20\lambda$  ( $D_2$  transition,  $\lambda = 780.2\text{nm}$ ,  $\Gamma = 2\pi \times 6\text{MHz}$  and  $I_{\text{sat}} \simeq 1.67\text{mW/cm}^2$ ). To isolate two internal states and obtain a cloud of two-level atoms, we apply a 50G-magnetic field oriented along a *radial* direction of the atomic cloud. The atoms are initially optically pumped to  $|g\rangle = |5S_{1/2}, F=2, m=2\rangle$ . To initiate a superradiant burst, we apply a pulse of resonant  $\sigma^+$ -polarized light to excite the atoms in  $|e\rangle = |5P_{3/2}, F=3, m=3\rangle$ . The excitation beam is sent along the magnetic field, *perpendicularly* to the elongated axis of the cloud. Its duration is 12 ns for a Rabi frequency  $\Omega \simeq 6.5\Gamma$ , limited by the available laser power. The excitation beam waist ( $100\mu\text{m}$ ) is much larger than the cloud dimensions, and the optical density of the cloud along the beam direction is negligible so that all atoms experience the same  $\Omega$ . The excitation pulse is temporally shaped with a combination of acousto- and electro-optical modulators, resulting in a turning on and off time of  $\simeq 1\text{ns}$ . The photons

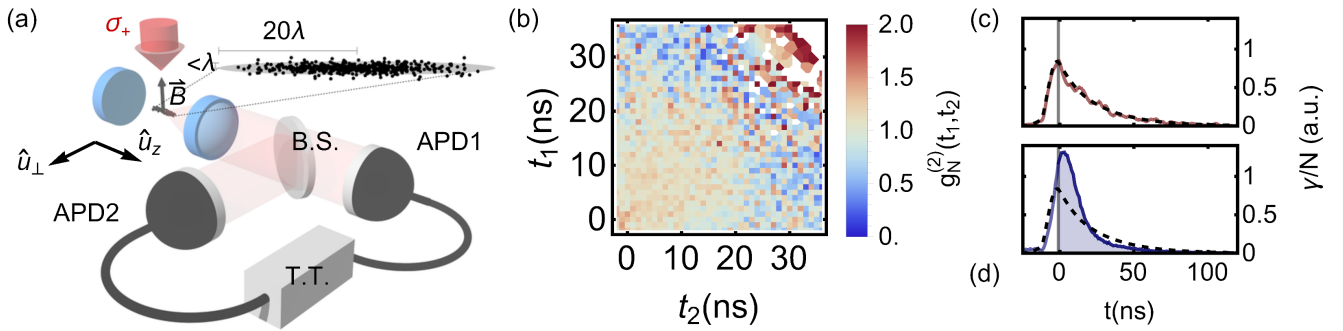


FIG. 1. (a) **Experimental setup:** an elongated cloud of  $^{87}\text{Rb}$  atoms, prepared in a dipole trap (not shown) is excited using a resonant laser beam propagating along a radial direction of the cloud. The light emitted in the diffraction pattern, along  $\mathbf{u}_z$ , is split by a 50/50 beamsplitter (BS) and sent onto two fibered avalanche photodiodes APD1,2. A time tagger (T.T.) records the photon arrivals times on each photodiode with respect to a common trigger. (b) Measurement of the two-times correlation function during the superradiant burst. (white part: absence of any measured coincidences) The number of repetitions is 30400, corresponding to about 10 hours of acquisition. (c,d) Photon emission rate collected in the  $\mathbf{u}_z$  direction for  $N \simeq 300$ (c) and  $N \simeq 3000$ (d), together with the solution of the Optical Bloch Equations (dashed black line). The vertical gray line indicates the end of the excitation pulse and the color-filled region in (d) indicates the temporal window where the intensity correlation is measured.

emitted by the cloud along its main axis ( $\mathbf{u}_z$  in Fig. 1(a)) are collected using fibered-coupled avalanches photodiodes (APDs).

The excitation is performed with the trapping laser turned off to eliminate the inhomogeneous broadening it induces. To accumulate enough statistics, the same atomic cloud is excited up to 100 times before a new ensemble is prepared and the whole sequence repeated a few hundred times. The fraction of atoms lost during the excitation does not exceed 10%. Given the temperature of the cloud, the atomic displacement  $\delta r$  during the excitation and the emission by the cloud is negligible (*i.e.*  $\delta r \ll 1/k$ ). We use an Hanbury-Brown and Twiss (HBT) configuration to measure the intensity correlation function  $g_N^{(2)}(t_1, t_2)$ : we split the collected light in two via a 50/50 fiber beamsplitter. We then measure in each arm the photon arrival time with respect to a common trigger. From these, we compute  $g_N^{(2)}(t_1, t_2) = n_c(t_1, t_2) / [n_1(t_1)n_2(t_2)]$  where  $n_i(t_k)$  is the photon number detected in arm  $i$  at time  $t_k$  and  $n_c(t_1, t_2)$  the number of coincidences on both arms at times  $t_1$  and  $t_2$ , as detailed in [26]. The minimum time bin we use is 1 ns. We present in Fig. 1(c) an example of two-times correlation function measured during a superradiant burst.

Figure 1 shows the photon emission rate  $\gamma(t)$  measured on APD1 for a cloud containing  $N \simeq 300$  (c) and  $N \simeq 3000$  (d) during and after the excitation pulse. The data are compared to the solution of the Optical Bloch Equations for a two-level atom (OBEs), including the measured temporal profile of the excitation laser. For low  $N$ , they are well reproduced by OBEs, indicating that the atoms are uncorrelated. In contrast, we observe a superradiant burst at large  $N$ , as we showed in [27]. For the Rabi frequency used and the finite temporal duration of the pulse, we reach a population inversion of about 85%, independent of  $N$  [27]. We stress that the cloud is excited perpendicularly to its long axis, so that, even for a non-perfect  $\pi$ -pulse, the laser does not impart any phase

coherence between the dipoles that could lead to an emission in the superradiant direction.

The main experimental result of this work is shown in Fig. 2, where we compare the photon emission rate and the equal time intensity correlation  $g_N^{(2)}(t, t)$ . This quantity is extracted from the two-times correlation function  $g_N^{(2)}(t_1, t_2)$ , considering  $t = t_1 = t_2$ , and integrating over a time-bin of 2 ns. We observe that the equal-time correlations decrease from  $\sim 1.5$  right after switching off the excitation light down to  $\sim 1$  after  $\simeq 15 \text{ ns} \simeq 1/2\Gamma$ . This behavior signs the spontaneous establishment of second-order coherence due to superradiance: at the begin of the superradiant emission, the emitters are still nearly independent, leading to  $g_N^{(2)}(t, t) > 1$ . Later, the progressive phasing of the dipoles during the superradiant emission results into an increasing second-order coherence, until  $g_N^{(2)}(t, t) \approx 1$ . Interestingly,  $g_N^{(2)}(t, t)$  reached up to 1.7 for  $t < 0$  and start to decay during the pulse itself: this is consistent with our previous finding [28] that superradiance starts to phase lock the dipoles even during the excitation. Finally, after a time  $\sim 2/\Gamma$ , the emission becomes subradiant, while the correlations remain close to 1.

In order to prove that the observed behavior is characteristic of the superradiant burst, we contrast it with the one where the atomic ensemble has reached steady-state under a constant drive, therefore preparing a different initial state. To do so, we apply the excitation laser with  $\Omega = 2\Gamma$  for a duration  $\simeq 120 \text{ ns}$ , long enough for the system to reach steady-state. We then measure  $g_N^{(2)}(t, t)$  after switching off of the driving laser, during the de-excitation process. From previous works, we know that the collective emission does not exhibit a burst but is rather characterized by a monotonous decay featuring mainly two time-scales [28, 29]: a first, superradiant one, faster than the natural decay time ( $\simeq 12 \text{ ns}$  in this specific case, compared to  $1/\Gamma \simeq 26 \text{ ns}$ ) and a slower, subradiant, one

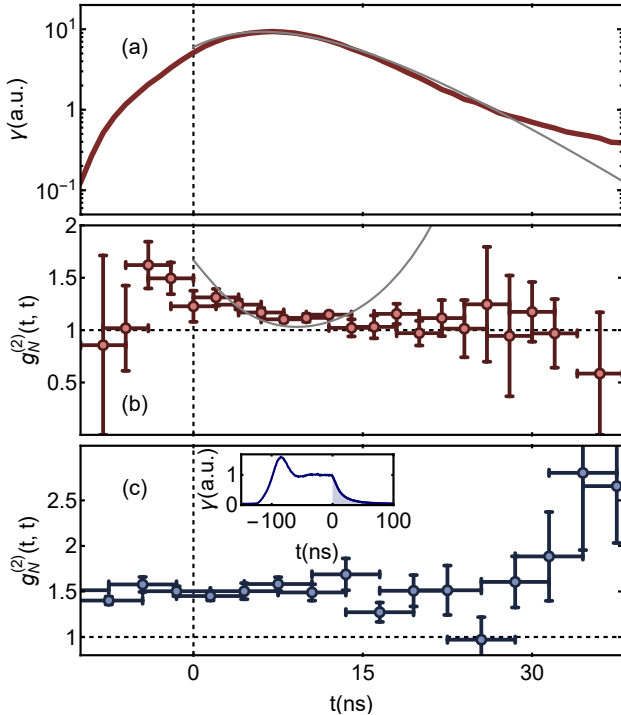


FIG. 2. **Statistics of the light emitted during a superradiant burst:** (a) red line: photon emission rate  $\gamma(t)$ , gray line prediction of DM (see text). (b) Red points: measured values of  $g_N^{(2)}(t,t)$  compared to the DM (gray line). Black dashed lines: guide to the eyes, indicating the end of the driving light ( $t=0$ ) and  $g_N^{(2)}(t,t)=1$ , in (b) and (c). Error bars in (b): for the y axes they correspond to the standard errors on the mean; for x-axes they account for the number of bins used in the averaging process. (c) Measurement of  $g_N^{(2)}(t,t)$  after the system reaches the steady-state. Error bars as in (b). Inset: temporal traces showing the coherent dynamics towards the steady state and the decay process (dashed region) where  $g_N^{(2)}(t,t)$  is measured.

( $\approx 47$  ns). [30]. As we showed in Ref. [26] (see also [31, 32]), atomic correlations are established during the drive and result into a *steady-state* value of the correlation  $g_{N,\text{st}}^{(2)}(0)$  lower than 2, the value expected for uncorrelated emitters. Figure 2(c) presents the result of the experiment: we observe that starting from  $g_N^{(2)}(0,0) = g_{N,\text{st}}^{(2)}(0)$ , the equal time intensity correlation remains constant until  $\sim 30$  ns, after which it increases. This trend deviates qualitatively and quantitatively from the one measured during the superradiant burst, indicating that the establishment of second-order temporal coherence is indeed related to the initial full inversion of the system leading to the burst.

As a guide to understand the experimental results, we compare them to the predictions of the Dicke model (DM) [2]. Briefly, the model considers  $N$  two-level emitters ( $|e\rangle$  and  $|g\rangle$ ) identically coupled to a single electromagnetic mode. This indistinguishability allows treating the system as a collective spin  $\hat{S}^+ = \sum_{i=1}^N \hat{\sigma}_i^+$ , where  $\hat{\sigma}_i^+ = |e\rangle\langle g|_i$  is the single atom

rising operator. If the initial state is symmetric with respect to the exchange of two atoms, as the fully excited one, this permutational invariance is preserved during the dynamics: the system is constraint to evolve in the symmetric subspace of dimension  $N+1$ . In the absence of an external driving, the collective emission is then governed by the following Lindblad equation:

$$\frac{d\hat{\rho}(t)}{dt} = \frac{\Gamma}{2} \left( 2\hat{S}^- \hat{\rho}(t) \hat{S}^+ - \hat{S}^+ \hat{S}^- \hat{\rho}(t) - \hat{\rho}(t) \hat{S}^+ \hat{S}^- \right) \quad (1)$$

which can be easily solved for  $\hat{\rho}(t)$ . The photon emission rate is  $\gamma(t) = \langle \hat{S}^+ \hat{S}^- \rangle = \text{Tr}[\hat{S}^+ \hat{S}^- \hat{\rho}(t)]$ . The equal time intensity correlation function is  $g_N^{(2)}(t,t) = \langle \hat{S}^+ \hat{S}^+ \hat{S}^- \hat{S}^- \rangle_t / \langle \hat{S}^+ \hat{S}^- \rangle_t^2 = \text{Tr}[\hat{S}^+ \hat{S}^+ \hat{S}^- \hat{S}^- \hat{\rho}(t)] / \text{Tr}[\hat{S}^+ \hat{S}^- \hat{\rho}(t)]^2$ . The DM assumes that all the atoms occupy a sub-wavelength volume, a condition far from being fulfilled experimentally. As shown in Ref. [2], in a mean-field approximation, the average dynamics of atomic observables is still described by Eq.(1) for an elongated sample by introducing an effective atom number  $\tilde{N} = \mu N$ , where the parameter  $\mu$  accounts for the coupling between the cloud and its diffraction mode [11, 29]. It depends only on the geometry of the cloud and in our case  $\mu \simeq 0.002$ , meaning that around  $\tilde{N} = 6$  atoms are cooperatively coupled to the diffraction mode. We report the prediction of the DM for  $\gamma(t)$  and  $g_N^{(2)}(t,t)$  as gray lines in Fig. 2(a,b). They describe the experimental trend during the first part of the dynamics, including the time-scale over which second-order coherence is established. We have not attempted to compare the data in Fig. 2(c) to the DM: although it should describe the decay, it is not valid during the laser excitation *perpendicular* to the main axis of the cloud, thus preventing us from calculating the atomic state in steady-state and the dynamics after the excitation is turned off.

Not surprisingly, however, we also observe discrepancies with respect to the predictions of the DM. First, the Dicke model predicts  $g_{N,\text{DM}}^{(2)}(0,0) = 2 - 2/\tilde{N} \approx 1.6$  [18]. This value is obtained considering a fully inverted initial state  $|e\rangle^{\otimes N} = |N/2, N/2\rangle$ . Experimentally, we measure a smaller value, which might be explained by the fact that the initial state exhibits partial coherence due to the establishment of superradiant correlations in a timescale faster than the  $\pi$ -pulse [27]. Second, we observe in Fig. 2(a) the appearance of subradiant decay at long-time, absent from the DM: As we found in previous works [28, 29], subradiant states are populated during the superradiant burst and during the  $\pi$  pulse. When subradiance dominates ( $t \gtrsim 1/\Gamma$ ), we observe that  $g_N^{(2)}(t,t) \approx 1$  while instead the DM predicts bunched correlations [9, 33, 34]: the second-order temporal coherence of our extended cloud is longer than the one predicted by Dicke's model. This failure of the DM is expected: the finite cloud size and light-induced dipole interactions break the permutational symmetry of the DM, leading to a finite coupling between bright and dark (subradiant) states [35].

Finally, and along the lines explored in Ref. [12], we plot in Fig. 3 the two-times correlation functions  $g^{(2)}(t_1, t_2)$  fixing

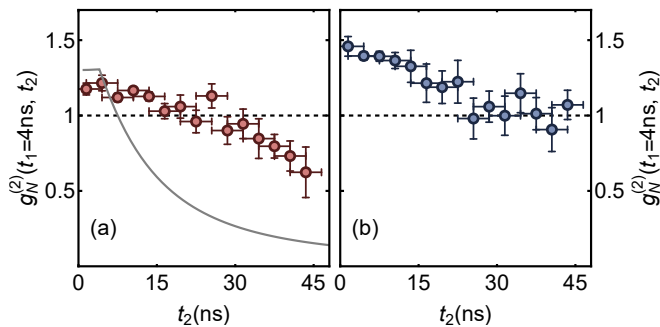


FIG. 3. (a) Intensity correlations  $g^{(2)}(t_1, t_2)$  at different times during a superradiant pulse, corresponding to a cut of the two-dimensional map shown in Fig. 1(b) for  $t_1 = 4$  ns (right). The gray lines is the predictions of the Dicke Model for  $\tilde{N} = 6$ , using the quantum regression theorem. (b) Same quantity measured during the decay following the steady-state excitation of the cloud, as in Fig. 2(c).

$t_1 = 4$  ns and varying the second time  $t_2$  (the observations below hold for different choices of  $t_1$ ). As found in Ref. [12], we observe here also the appearance of anti-correlations after  $|t_1 - t_2| \sim 25$  ns  $\sim 1/\Gamma$ . As noted in Ref. [12], one can interpret these anti-correlations as stemming from the fact that the superradiant burst emitted at each realization, triggered by a spontaneous emission at a random time, is shorter than the average intensity shown in Fig. 1(d) [2]. More generally, as the photon number  $\sum_t n_1(t) = \sum_t n_2(t) = N_{\text{ph}}$  emitted during the pulse following full inversion is fixed, the observation of bunching implies that anti-correlations should be observed: Indeed,  $\sum_{t,t'} n_c(t, t') = N_{\text{ph}}(N_{\text{ph}} - 1) \simeq N_{\text{ph}}^2$  and  $\sum_{t,t'} n_1(t)n_2(t') = N_{\text{ph}}^2$  lead to  $\sum_{t,t'} n_1(t)n_2(t')g^{(2)}(t, t') = \sum_{t,t'} n_1(t)n_2(t')$ , from which we conclude that  $g^{(2)}(t, t') > 1$  results into  $g^{(2)}(t, t') < 1$  for some  $t \neq t'$ . The quantitative predictions of the DM (using the quantum regression theorem [36]) are also reported in Fig. 3(a): they reproduce the general trend, but fail to give the timescale, calling for a better model. Finally, we plot  $g^{(2)}(t_1, t_2)$  during the decay following the excitation of the cloud into a steady-state (Fig. 2c). There, we do not observe the appearance of clear anti-correlations: the argument presented above is indeed only valid when  $N_{\text{ph}}$  is the same for each repetition of the experiment. This is the case for a full inversion of the system leading to a superradiant burst, but not when preparing an atomic steady state, which is a mixed superposition of super and sub-radiant states containing various numbers of excited atoms: there, the number of emitted photons varies from shot-to-shot.

In conclusion, we have measured the two-times intensity correlation function during a superradiant burst emitted by an elongated atomic cloud, and observed the establishment of second-order temporal coherence. The early dynamics of the correlations is reproduced by the Dicke model introducing an effective atom number to account for the finite size. We have also observed the limit of the model, which does not capture the subradiant decay at long-time. This poses the theoretical

challenge of a microscopic description of the system [21, 37, 38]. Our work suggests the investigation of the intensity correlations also in the *driven* Dicke model [20], where they are expected to oscillate at twice the Rabi frequency deeply in the superradiant phase [39, 40], a hallmark of collective behavior. Another direction is related to the study of directional effects in the photon statistics, which might reveal the many-body nature of the emission [18, 41], or the investigation of higher-order correlation functions [42]

We acknowledge discussions with M. Fleischhauer, C. Mink, P. Schneeweiss, A. Rauschenbeutel and their team. We thank A. Glicenstein for assistance in the early stages of the experiment. This project has received funding from the European Research Council (Advanced grant No. 101018511, ATARAXIA), by the Agence Nationale de la Recherche (ANR, project DEAR and ANR-22-PETQ-0004 France 2030, project QuBitAF).

\* feroli@lens.unifi.it

† igor.ferrier-barbut@institutoptique.fr

‡ antoine.browaeys@institutoptique.fr

- [1] R. H. Dicke, Coherence in spontaneous radiation processes, *Phys. Rev.* **93**, 99 (1954).
- [2] M. Gross and S. Haroche, Superradiance: An essay on the theory of collective spontaneous emission, *Physics Reports* **93**, 301 (1982).
- [3] N. Skribanowitz, I. P. Herman, J. C. MacGillivray, and M. S. Feld, Observation of dicke superradiance in optically pumped hf gas, *Phys. Rev. Lett.* **30**, 309 (1973).
- [4] M. Gross, C. Fabre, P. Pillet, and S. Haroche, Observation of near-infrared dicke superradiance on cascading transitions in atomic sodium, *Phys. Rev. Lett.* **36**, 1035 (1976).
- [5] H. M. Gibbs, Q. H. F. Vrethen, and H. M. J. Hikspoors, Single-pulse superfluorescence in cesium, *Phys. Rev. Lett.* **39**, 547 (1977).
- [6] R. Röhlsberger, K. Schlage, B. Sahoo, S. Couet, and R. Ruffer, Collective lamb shift in single-photon superradiance, *Science* **328**, 1248 (2010).
- [7] J. A. Mlynek, A. A. Abdumalikov, C. Eichler, and A. Wallraff, Observation of dicke superradiance for two artificial atoms in a cavity with high decay rate, *Nature communications* **5**, 5186 (2014).
- [8] C. Liedl, F. Tebbenjohanns, C. Bach, S. Pucher, A. Rauschenbeutel, and P. Schneeweiss, Observation of superradiant bursts in a cascaded quantum system, *Phys. Rev. X* **14**, 011020 (2024).
- [9] F. Jahnke, C. Gies, M. Aßmann, M. Bayer, H. Leymann, A. Foerster, J. Wiersig, C. Schneider, M. Kamp, and S. Höfling, Giant photon bunching, superradiant pulse emission and excitation trapping in quantum-dot nanolasers, *Nature communications* **7**, 11540 (2016).
- [10] D. C. Gold, P. Huft, C. Young, A. Safari, T. G. Walker, M. Saffman, and D. D. Yavuz, Spatial coherence of light in collective spontaneous emission, *PRX Quantum* **3**, 010338 (2022).
- [11] F. Tebbenjohanns, C. D. Mink, C. Bach, A. Rauschenbeutel, and M. Fleischhauer, [Predicting correlations in superradiant emission from a cascaded quantum system](#) (2024),

- arXiv:2407.02154 [quant-ph].
- [12] C. Bach, F. Tebbenjohanns, C. Liedl, P. Schneeweiss, and A. Rauschenbeutel, *Emergence of second-order coherence in superfluorescence* (2024), arXiv:2407.12549 [quant-ph].
- [13] F. Haake, M. I. Kolobov, C. Fabre, E. Giacobino, and S. Reynaud, Superradiant laser, *Phys. Rev. Lett.* **71**, 995 (1993).
- [14] J. G. Bohnet, Z. Chen, J. M. Weiner, D. Meiser, M. J. Holland, and J. K. Thompson, A steady-state superradiant laser with less than one intracavity photon, *Nature* **484**, 78 (2012).
- [15] K. Debnath, Y. Zhang, and K. Mølmer, Lasing in the superradiant crossover regime, *Phys. Rev. A* **98**, 063837 (2018).
- [16] T. Maier, S. Kraemer, L. Ostermann, and H. Ritsch, A superradiant clock laser on a magic wavelength optical lattice, *Opt. Express* **22**, 13269 (2014).
- [17] O. Tziperman, A. Gorlach, R. Ruimy, N. Gutman, C. Mechel, G. Baranes, A. Pizzi, and I. Kaminer, Engineering quantum states of light using superradiance, in *CLEO 2023* (Optica Publishing Group, 2023) p. FM1E.6.
- [18] S. J. Masson, I. Ferrier-Barbut, L. A. Orozco, A. Browaeys, and A. Asenjo-Garcia, Many-body signatures of collective decay in atomic chains, *Phys. Rev. Lett.* **125**, 263601 (2020).
- [19] F. Haake and R. J. Glauber, Quantum statistics of superradiant pulses, *Phys. Rev. A* **5**, 1457 (1972).
- [20] G. Ferioli, A. Glicenstein, I. Ferrier-Barbut, and A. Browaeys, A non-equilibrium superradiant phase transition in free space, *Nature Physics*, **1** (2023).
- [21] C. D. Mink and M. Fleischhauer, Collective radiative interactions in the discrete truncated wigner approximation, *SciPost Phys.* **15**, 233 (2023).
- [22] O. Rubies-Bigorda, S. Ostermann, and S. F. Yelin, Characterizing superradiant dynamics in atomic arrays via a cumulant expansion approach, *Phys. Rev. Res.* **5**, 013091 (2023).
- [23] O. Rubies-Bigorda and S. F. Yelin, Superradiance and subradiance in inverted atomic arrays, *Phys. Rev. A* **106**, 053717 (2022).
- [24] F. Robicheaux, Theoretical study of early-time superradiance for atom clouds and arrays, *Phys. Rev. A* **104**, 063706 (2021).
- [25] A. Glicenstein, G. Ferioli, L. Brossard, Y. R. P. Sortais, D. Barredo, F. Nogrette, I. Ferrier-Barbut, and A. Browaeys, Preparation of one-dimensional chains and dense cold atomic clouds with a high numerical aperture four-lens system, *Phys. Rev. A* **103**, 043301 (2021).
- [26] G. Ferioli, S. Pancaldi, A. Glicenstein, D. Clément, A. Browaeys, and I. Ferrier-Barbut, Non-gaussian correlations in the steady state of driven-dissipative clouds of two-level atoms, *Phys. Rev. Lett.* **132**, 133601 (2024).
- [27] G. Ferioli, A. Glicenstein, F. Robicheaux, R. T. Sutherland, A. Browaeys, and I. Ferrier-Barbut, Laser-driven superradiant ensembles of two-level atoms near dicke regime, *Phys. Rev. Lett.* **127**, 243602 (2021).
- [28] A. Glicenstein, G. Ferioli, A. Browaeys, and I. Ferrier-Barbut, From superradiance to subradiance: exploring the many-body dicke ladder, *Optics Letters* **47**, 1541 (2022).
- [29] G. Ferioli, A. Glicenstein, L. Henriët, I. Ferrier-Barbut, and A. Browaeys, Storage and release of subradiant excitations in a dense atomic cloud, *Phys. Rev. X* **11**, 021031 (2021).
- [30] For the specific parameters chosen here, a few percent of the total excitation are stored in the subradiant modes.
- [31] P. Lassègues, M. A. F. Biscassi, M. Morisse, A. Cidrim, N. Matthews, G. Labeyrie, J.-P. Rivet, F. Vakili, R. Kaiser, W. Guerin, *et al.*, Field and intensity correlations: the siegert relation from stars to quantum emitters, *The European Physical Journal D* **76**, 246 (2022).
- [32] P. Lassègues, M. A. F. Biscassi, M. Morisse, A. Cidrim, P. G. S. Dias, H. Eneriz, R. C. Teixeira, R. Kaiser, R. Bachelard, and M. Hugbart, Transition from classical to quantum loss of light coherence, *Phys. Rev. A* **108**, 042214 (2023).
- [33] D. Bhatti, J. von Zanthier, and G. S. Agarwal, Superbunching and nonclassicality as new hallmarks of superradiance, *Scientific reports* **5**, 17335 (2015).
- [34] Q.-u.-A. Gulfam and Z. Ficek, Highly directional photon superbunching from a few-atom chain of emitters, *Phys. Rev. A* **98**, 063824 (2018).
- [35] A. Cipris, N. A. Moreira, T. S. do Espirito Santo, P. Weiss, C. J. Villas-Boas, R. Kaiser, W. Guerin, and R. Bachelard, Subradiance with saturated atoms: Population enhancement of the long-lived states, *Phys. Rev. Lett.* **126**, 103604 (2021).
- [36] D. A. Steck, Quantum and atom optics, (2007).
- [37] S. Agarwal, E. Chaparro, D. Barberena, A. P. Orioli, G. Ferioli, S. Pancaldi, I. Ferrier-Barbut, A. Browaeys, and A. Rey, Directional superradiance in a driven ultracold atomic gas in free-space, arXiv preprint arXiv:2403.15556 (2024), arXiv:2403.15556 [cond-mat.quant-gas].
- [38] D. Goncalves, L. Bombieri, G. Ferioli, S. Pancaldi, I. Ferrier-Barbut, A. Browaeys, E. Shahmoon, and D. E. Chang, Driven-dissipative phase separation in free-space atomic ensembles, (2024), arXiv:2403.15237 [quant-ph].
- [39] G. S. Agarwal, L. M. Narducci, D. H. Feng, and R. Gilmore, Intensity correlations of a cooperative system, *Phys. Rev. Lett.* **42**, 1260 (1979).
- [40] S. S. Hassan, G. P. Hildred, R. R. Puri, and S. V. Lawande, Non-resonant effects in the fluorescent dicke model. ii. semiclassical and quantal results, *Journal of Physics B: Atomic and Molecular Physics* **15**, 1029 (1982).
- [41] S. Cardenas-Lopez, S. J. Masson, Z. Zager, and A. Asenjo-Garcia, Many-body superradiance and dynamical mirror symmetry breaking in waveguide qed, *Phys. Rev. Lett.* **131**, 033605 (2023).
- [42] N. Stiesdal, J. Kumlin, K. Kleinbeck, P. Lunt, C. Braun, A. Paris-Mandoki, C. Tresp, H. P. Büchler, and S. Hofferberth, Observation of three-body correlations for photons coupled to a rydberg superatom, *Phys. Rev. Lett.* **121**, 103601 (2018).